AIAA 91-0236
Interaction of Vorticity with a Free Surface in Turbulent Open Channel Flow

R.I. Leighton†, T.F. Swean, Jr., R.A. Handler, and J.D. Swearingen

Center for Advanced Space Sensing,
Naval Research Laboratory,
Washington, D.C.

†Science Applications International Corp.,
McLean, Va.

29th Aerospace Sciences Meeting
January 7-10, 1991/Reno, Nevada

DISCLAIMER NOTICE

THIS DOCUMENT IS BEST QUALITY PRACTICABLE. THE COPY FURNISHED TO DTIC CONTAINED A SIGNIFICANT NUMBER OF PAGES WHICH DO NOT REPRODUCE LEGIBLY.

INTERACTION OF VORTICITY WITH A FREE SURFACE IN TURBULENT OPEN CHANNEL FLOW

R.I. Leighton*, T.F. Swean, Jr.†, R.A. Handler,+ J.D. Swearingen+

Center For Advanced Space Sensing
Naval Research Laboratory
Washington, D.C. 20375-5000

Abstract

The interaction between vorticity and a free surface, modeled as a shear free boundary is studied using a direct numerical simulation of an open channel flow at low Reynolds number ($Re_{fT} = U_f h/\nu = 2340$ where h is the channel depth and U_{fT} is the mean free-surface velocity). As a result of the shear free nature of the top boundary, only normal vorticity may terminate on it. The vorticity components parallel to the top boundary must go to zero as the boundary is approached. The time averaged fluctuating enstrophy balance equations, which are an indicator of the level of activity of the vorticity field are evaluated. Near the free surface the rate of production and destruction of enstrophy is set by the stretching and rotation of fluctuating vorticity by the fluctuating velocity field. The transport of enstrophy by the fluctuating velocity has a minor role. Of the the production terms, the three involving the stretching of vorticity along its axis are the most important, and a simple model explaining this is presented.

(25) * Vortices, * Turbulent flow, * channel flow.

Nomenclature

U_i	Instantaneous velocity
u_i	Fluctuating velocity
Ω_i	Instantaneous vorticity
ω_i	Fluctuating vorticity
$u_i' = \sqrt{\sum_{x_1,x_3} u_i^2}$	RMS fluctuating velocity
$\omega_i' = \sqrt{\sum_{x_1,x_3} \omega_i^2}$	RMS fluctuating vorticity
$\overline{U_i}(x_2)$	Mean velocity
$U_f = \overline{U_1}(x_2 = 0.0)$	Mean free surface velocity
$u^* = \sqrt{\tau_{wall}/\rho}$	Friction velocity
$l^* = \nu/u^*$	Viscous lengthscale
$t^* = \nu/u^{*2}$	Viscous timescale
$u_i^+ = u_i/u^*$	Non-dimensional velocity
$l_i^+ = l_i/l^*$	Non-dimensional length
$t^+ = t/t^*$	Non-dimensional time
$\langle a(\mathbf{x})\rangle = \sum_{ensemble} a(\mathbf{x})$	Averaging operator
$h = L_{x_2}$	Channel height
L_{x_1}	Streamwise box length
L_{x_3}	Transverse box length
ν	Kinematic viscosity
ρ	density
$Fn = U_f/\sqrt{gh}$	Froude number
$Re = Uh/\nu$	Reynolds number
$Re^* = u^* h/\nu$	Wall Reynolds number
$Re_f = U_f h/\nu$	Free surface Reynolds no.

1. Introduction

The total instantaneous enstrophy of a fluid is defined as the square of the instantaneous vorticity, $\sum_i \Omega_i\Omega_i$. Enstrophy can be determined as well from the mean vorticity, $\overline{\Omega_i}\overline{\Omega_i}$, and the fluctuating vorticity, $\overline{\omega_i\omega_i}$. This paper will be limited to an analysis of the fluctuating vorticity. The dominate motivation for studying the enstrophy balance equations is the natural interpretation of enstrophy as a measure of vortical activity. The no-slip boundary, where the majority of the fluctuating vorticity is produced is the source of the turbulent kinetic energy. Much of the turbulent kinetic energy is believed to be associated with coherent structures and a quasi-regular turbulent burst cycle. If it is assumed that coherent vorticity is an important feature of these structures, then enstrophy is a good tool for analysis. Although a clear connection between vorticity and coherent structures or events has yet to be developed, the concept of the vortex loop has often invoked to explain the visualization of the results of experiments or direct numerical simulations (DNS). The connection between vorticity and turbulent structures may be equally valid at the free-surface. As will be discussed below, the conditions at the free-surface require that vorticity tangential to the surface vanish as the surface is approached. Simultaneously, the surface-normal gradient of the component of vorticity perpendicular to the surface must vanish. These are reflectional boundary conditions, and are significantly different than the

*Research Scientist, SAIC, McLean, VA, 22102
†Research Mechanical Engineer, NRL, Member AIAA
+Mechanical Engineer, NRL

condition of rotational symmetry about the x_1-axis (aligned with the channel centerline) that occurs in the closed channel case.

Another important interpretation of enstrophy can be made through its relation to the isotropic dissipation function. The isotropic dissipation function, commonly used in $k-\epsilon$ turbulence models, is defined as:

$$\epsilon = \nu \overline{\frac{\partial u_i}{\partial x_j}\frac{\partial u_i}{\partial x_j}}, \tag{1}$$

for homogeneous turbulence. However, the following can be shown

$$\begin{aligned}\overline{\frac{\partial u_i}{\partial x_j}\frac{\partial u_i}{\partial x_j}} &= \frac{1}{2}\overline{\frac{\partial u_i}{\partial x_j}\frac{\partial u_i}{\partial x_j}} + \frac{1}{2}\overline{\frac{\partial u_j}{\partial x_i}\frac{\partial u_j}{\partial x_i}} \\ &= \frac{1}{2}\overline{(\frac{\partial u_i}{\partial x_j} - \frac{\partial u_j}{\partial x_i})(\frac{\partial u_i}{\partial x_j} - \frac{\partial u_j}{\partial x_i})} \\ &= \overline{\omega_k\omega_k}.\end{aligned} \tag{2}$$

In Eq. 2 the identity for homogeneous incompressible turbulence,

$$\begin{aligned}\overline{\frac{\partial u_i}{\partial x_j}\frac{\partial u_j}{\partial x_i}} &= \frac{\partial}{\partial x_j}\overline{(u_i\frac{\partial u_i}{\partial x_j})} - \overline{u_i(\frac{\partial}{\partial x_j}\frac{\partial u_i}{\partial x_j})} \\ &= 0,\end{aligned} \tag{3}$$

has been used[1]. Therefore the isotropic dissipation function is related to the fluctuating enstrophy as

$$\epsilon = \nu\overline{\omega_k\omega_k}. \tag{4}$$

Consequently, the study of the enstrophy balance can be viewed as the study of the creation and destruction of the isotropic dissipation function. The enstrophy balance equation may be a more convenient tool to study the dissipation because its terms have better physical interpretations. Furthermore the component equations $\omega_i\omega_i$ (no implied summation) can be examined individually. As mentioned above, while the isotropic dissipation is not the local dissipation of turbulent kinetic energy, it is relevent for turbulence modeling.

2. The Numerical Simulation

The incompressible three-dimensional Navier-Stokes equations are solved for initial and boundary conditions approximating a turbulent open-channel flow of water at a Reynolds number of 2340, where $Re_h = U_f h/\nu$ and h is the channel depth and U_f,

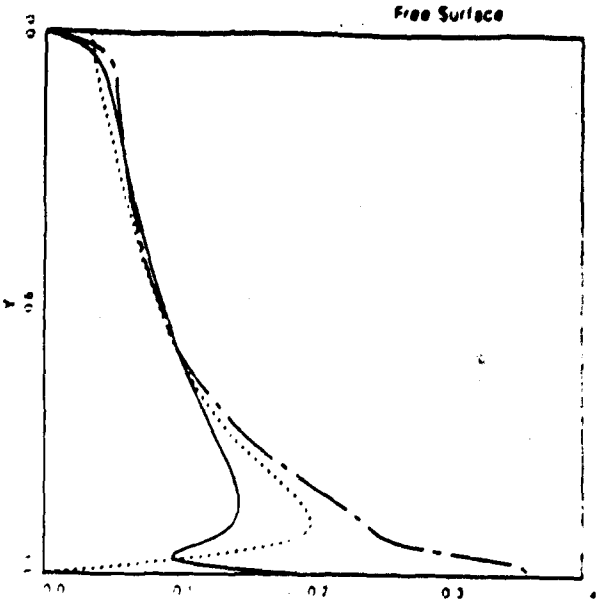

Fig. 1 RMS Fluctuating Vorticity.Symbols: —— ω_1'; — · — ω_2'; - - - - ω_3'.

is the mean free-surface velocity. Based on the friction velocity, $u_* = \sqrt{\frac{\tau_{wall}}{\rho}}$, the Reynolds number is $Re_* = 134$. The governing equations are recast into a 4^{th} order equation for the vertical velocity and a 2^{nd} order equation for the vertical vorticity and the continuity equation is solved explicitly in the recovery of the streamwise velocity. This formulation was first discussed by Orszag and Patera[2] and later implemented in a simpler form in the large scale direct simulations by Kim, Moin and Moser[3]. It is the latter formulation that will be used. This method involves the use of the homogeneous solutions of the time discretized 4^{th} order equation to satisfy all the required boundary conditions. The equations are numerically solved after they are Fourier transformed in the streamwise (x_1) and spanwise (x_3) directions and Chebychev transformed in the vertical direction (x_2). The x_2 axis, scaled by the channel height has its origin at the free surface. The channel bottom is $x_2 = -1$. The calculations are performed on a grid of $48\times65\times64$ nodes in x_1, x_2, x_3, respectively, for a resolution of $26.3l_*$ in the streamwise direction and $13.2l_*$ in the spanwise direction ($l_* = \nu\sqrt{\frac{\rho}{\tau_{wall}}}$). The total box size is $1684l_* \times 134l_* \times 632l_*$. With the geometry scaled by the channel height, the height, length and width of the channel are 1, 4π and $3\pi/2$, respectively.

In the free-surface problem the nonlinear and time-dependent boundary conditions must be satisfied on an unknown surface elevation, η. The boundary conditions can be simplified considerably if the surface is not allowed to deflect ($\eta \equiv 0$). The

lid approximation is equivalent to

$$u_2 = 0 \text{ at } x_2 = 0. \tag{5}$$

To further simplify the boundary conditions, the usual balance of normal stresses[6] is replaced by

$$\frac{\partial^2 u_2}{\partial x_2^2} = 0 \text{ at } x_2 = 0. \tag{6}$$

Eq. 6 can be derived from the zero tangential stress conditions, the continuity equation, and the rigid lid assumption. These conditions and the definition of vorticity can also be combined to form the remaining free-surface boundary condition,

$$\frac{\partial \omega_2}{\partial x_2} = 0 \text{ at } x_2 = 0, \tag{7}$$

where the vorticity is non-dimensionalized by U_0/h. U_0 is the initial ($t = 0$) free-surface velocity.

At the bottom wall of the channel, the no-slip velocity boundary conditions are composed. The no-slip velocity condition sustains the shear layer which is responsible for maintaining the turbulence. The boundary conditions are periodic on all dependent variables in the streamwise and spanwise directions.

After the wall shear stress achieved a statistically steady state at the correct value, and the total stress across the channel was linear, turbulent flow data was acquired. Forty-two realizations of the turbulent flow were saved during an interval of approximately $4000t^*$ ($t^* = \nu/u^{*2}$). We have compared single point statistics and spectra with from the closed channel calculation performed at the Naval Research Laboratory[7] and, where possible, results from the high resolution NASA Ames closed channel computation[3]. In general, the single point statistics in the wall and buffer regions are very similar to the closed channel results. The effects of the upper boundary are apparent in the range of $0.0 \leq x_2 \leq -0.3$ as compared to similar data from the closed channel calculations.

3. Fluctuating Vorticity

The near wall behavior of the rms vorticity, ω_i' in Fig. 1 is similar to the prior results of Kim, Moin and Moser[3]. Near the free surface the horizontal components of vorticity vanish, while the vertical component approaches a constant value of $\omega_2'\nu/u^{*2} = 0.035$. This can be compared to 0.057 at the centerline for a low resolution closed channel simulation performed at NRL and 0.042 for the results Kim, Moin and Moser[3]. A Taylor series expansion about the top boundary indicates that ω_1' and ω_3' both approach zero linearly. A physical explanation of why $|\frac{d\omega_1'}{dx_2}| > |\frac{d\omega_3'}{dx_2}|$ as the free surface is being approached can be developed by examining the $\overline{\omega_i\omega_i}$ balance equations.

4. Balance Equations

The relationship of enstrophy to fluctuating vorticity is similar to the relationship of turbulent kinetic energy to fluctuating velocity. The balance equations are derived in the same manner as the balance equations for the components of the Reynolds stress tensor. The equations for the mean and instantaneous vorticity are multiplied the mean and instantaneous vorticity, respectively. These equations are time averaged resulting in equations for the mean enstrophy and the mean equation of the instantaneous enstrophy. Subtracting the latter from the former yields the equation of the mean fluctuating enstrophy. As in the case of the Reynolds stress tensor, the equations for the individual components of the enstrophy $\overline{\omega_1\omega_1}, \overline{\omega_2\omega_2}, \overline{\omega_3\omega_3}$ can be formulated. The details of the derivation of the balance equation for the fluctuating enstrophy are contained in Balint, Vukoslavcevic and Wallace[4]. The steady state balance equations are:

$$\begin{aligned} \overline{U_j}\frac{\partial}{\partial x_j}\left(\frac{1}{2}\overline{\omega_i\omega_i}\right) = &-\overline{u_j\frac{\partial}{\partial x_j}\left(\frac{1}{2}\omega_i\omega_i\right)} - \overline{u_j\omega_i}\frac{\partial \overline{\Omega}_i}{\partial x_j} \\ &+\overline{\omega_i\omega_j}\frac{\partial \overline{U}_i}{\partial x_j} + \overline{\omega_i\omega_j\frac{\partial u_i}{\partial x_j}} \\ &+\overline{\Omega}_j\overline{\omega_i\frac{\partial u_i}{\partial x_j}} + \nu\frac{\partial^2 \frac{1}{2}\overline{\omega_i\omega_i}}{\partial x_j^2} - \nu\overline{\frac{\partial \omega_i}{\partial x_j}\frac{\partial \omega_i}{\partial x_j}}, \end{aligned} \tag{8}$$

with $i = 1, 2$ or, 3 for the component equations and an implied summation for the total fluctuating enstrophy.

According to Tennekes and Lumley[5] and Balint et al., the eight terms of the enstrophy balance equation have the following interpretation:

(1) $\overline{U_j}\frac{\partial}{\partial x_j}\left(\frac{1}{2}\overline{\omega_i\omega_i}\right)$: The convection of the fluctuating enstrophy,

(2) $-\overline{u_j\frac{\partial}{\partial x_j}\left(\frac{1}{2}\omega_i\omega_i\right)}$: Transport of fluctuating enstrophy by fluctuating velocity,

(3) $-\overline{u_j\omega_i}\frac{\partial \overline{\Omega}_i}{\partial x_j}$: Gradient production of enstrophy,

(4) $\overline{\omega_i\omega_j}\frac{\partial \overline{U}_i}{\partial x_j}$: production by mean velocity gradient,

(5) $\overline{\omega_i\omega_j\frac{\partial u_i}{\partial x_j}}$: production by fluctuating velocity gradient.

(6) $\overline{\Omega}_j\overline{\omega_i\frac{\partial u_i}{\partial x_j}}$: Mixed production,

(7) $\nu\frac{\partial^2 \frac{1}{2}\overline{\omega_i\omega_i}}{\partial x_j^2}$: Viscous diffusion,

(8) $\nu\overline{\frac{\partial \omega_i}{\partial x_j}\frac{\partial \omega_i}{\partial x_j}}$: Viscous dissipation.

The interpretation of terms 1 – 6 can be expanded by examining the non-linear term of the vorticity equation from which they were derived:

$$\nabla \times \mathbf{u} \times \boldsymbol{\omega} = (\boldsymbol{\omega}\cdot\nabla)\mathbf{u} - (\mathbf{u}\cdot\nabla)\boldsymbol{\omega}.$$

The first term is the amount of instantaneous stretching or rotation of the vorticity by the gradient of the velocity field. Following Batchelor[6], if P and Q are two local points on a vortex line, then

$$(\omega \cdot \nabla)\mathbf{u} = |\omega| \lim_{PQ \to 0} \frac{\delta \mathbf{u}}{PQ}, \qquad (11)$$

where δu is the variation u over the distance PQ. That component of δu which is aligned with ω acts to stretch or compress the vorticity while the component perpendicular to ω causes the vortex line to undergo instantaneous rigid body rotation. For example if we assume the vorticity is aligned in the x_3 direction then

$$\omega_3 \frac{\partial u_1}{\partial x_3}$$

is the rotation of the vorticity vector from the ω_3 component to the ω_1. A similar interpretation holds for $\omega_3 \frac{\partial u_2}{\partial x_3}$. In the remaining direction the vorticity and the velocity gradient are aligned and stretching or compressing of the vorticity occurs. This is shown in Fig. 2. The second term on the right hand side of equation (10) is the convective part of the substantial derivative.

Terms (1), (2), and (3) of Eq. 8 can be identified with the convective part of the nonlinear terms: (1) and (2) can be considered as transport terms and (3) being a gradient production term. For the geometry under study term (1), transport by the mean velocity is zero. Terms (4), (5) and (6) are stretching/compression/rotation terms. Term (4) accounts for the production of $\overline{\omega_1 \omega_1}$ due to the rotation of ω_2 into ω_1 by $\frac{\partial U_1}{\partial x_2}$. This term, which is non-zero only for $i = 1$, and $j = 2$ represents the action of the mean velocity on the fluctuating vorticity. Term (5) is the production of enstrophy due to the stretching/compression and rotation of fluctuating vorticity by the fluctuating velocity field. As will be shown later, this is an important term near the free-surface. Term (6), the so-called mixed production term accounts for the production of enstrophy due to the stretching and rotation of the mean vorticity field, $\overline{\Omega}_3$, by the fluctuating velocity fields, u_i. This term represents the action of the fluctuating velocity field on the mean vorticity field. The last two terms are interpreted as viscous diffusion and viscous dissipation of fluctuating enstrophy.

5. The Enstrophy Balances

The terms of Eq. (8) have been calculated and are shown in Fig. 3. They are normalized by the initial free-surface velocity and the channel height. The balance for the total enstrophy and its components near the free surface are in Figs. 4 a-d. Gains in enstrophy are indicated on the right hand side of these figures. The individual terms give a better indication of the mechanisms by which the enstrophy is generated and destroyed. Note that the scale of the abscissa has been changed between Fig. 4a and Figs 4b-d.

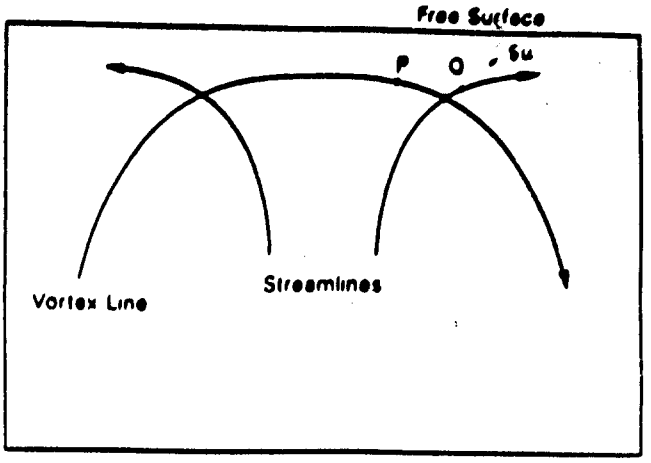

Fig. 2. A schematic of vortex stretching and rotation by the fluctuating velocity.

5.1 Balance Near the Wall

The majority of the production and dissipation of vorticity fluctuations occurs near the wall where the mean velocity gradient and the mean spanwise vorticity are large. In a very thin region near the wall the diffusion and dissipation of enstrophy are in balance. In the region ($-0.8 \geq x_2 \geq -0.95$) the mixed production term (6), the production by the mean velocity gradient term (4), and the turbulent production terms (5) are the dominate sources for fluctuating enstrophy, in increasing importance away from the wall. These terms are the rotation/stretching terms of the balance equations. The gains are almost completely balanced by the viscous dissipation. The transport/convection related terms are all small. With the exception of near the free surface, the terms of the individual balances decrease with increasing distance from the wall. Near the free-surface there is a thin region ($x_2 \geq -0.10$) of significant change. Details of the individual balances near the wall can be found in Leighton, et al.[7].

5.2 Balance Near the Surface

As can be seen in Fig. 4a, the viscous dissipation of enstrophy (8) and the turbulent production (5) dominate in the region $-0.10 \geq x_2 \geq -0.33$. In this region there is still some production of fluctuating enstrophy by the mean velocity gradient. Since the mean velocity gradient must approach zero at a free shear free surface, the enstrophy production due to the mean gradient must go to zero. Turbulent production of enstrophy, the dominate production mechanism for the upper 1/3 of the channel decays rapi-

for $x_2 > -0.05$. Viscous diffusion and turbulent transport act to increase the enstrophy in the region $x_2 > -0.10$. Enstrophy dissipation balances the production and diffusion near the top boundary. In the thin region $y \geq -0.08$ the significant changes in the terms of Eq. 8 can be understood by examining the component terms.

Figs. 4b-d show the level of gain or loss for each component of enstrophy near the surface. In the upper 1/3 of the channel the transport term becomes relatively more important, albeit the term is still small. The fluctuating normal velocity field transports $\omega_1\omega_1$ and $\omega_3\omega_3$ towards the surface. As the gradients in ω_1' and ω_3' increase near the surface, there is a corresponding increase in the enstrophy transport (see Fig. 1). The action of the transport term of $\omega_2\omega_2$, while always small, is to reduce the level of normal vorticity near the surface.

Figs. 4b and 4c show that the mixed production terms do play a role in the top of the channel, but approach zero as the shear-free surface is approached. It is interesting to note that the mixed production term for the $\overline{\omega_1\omega_1}$ balance equation is negative in the region $(0.0 \geq y \geq -0.33)$ and almost completely balanced by the production due to the mean velocity gradient. In the case of $\overline{\omega_1\omega_1}$, this term expresses the effect of the rotation of the mean vorticity vector by the fluctuating velocity field to cancel the fluctuating axial vorticity. This is done at nearly the same rate at which vorticity is being rotated out of the mean vorticity into the fluctuating normal vorticity by the fluctuating normal velocity.

The dissipation and diffusion curves in Figs. 4b-d indicates a strong dependence of the diffusion and dissipation process on the orientation of the vorticity. Viscous diffusion, which has been negligible in the region $-0.1 \geq y \geq -0.85$ becomes the dominate source for the horizontal components of enstrophy ($\omega_1\omega_1$ and $\omega_3\omega_3$) near the surface, $(y \geq -0.05)$. Due to the reflective nature of the shear free boundary, the horizontal components of vorticity go to zero at the boundary and any such vorticity near the boundary will be influenced by the anti-parallel image vorticity. The effect of the image vorticity or equivalently the shear-free boundary is to increase diffusion of the vorticity in the fluid towards its image, and in the process increase the dissipation of enstrophy. For the normal component ($\omega_2\omega_2$) the process of dissipation and diffusion are entirely different. In this case the image vorticity is not anti-parallel vorticity promoting diffusion, but simply a continuation of the physical vorticity across the shear-free interface. The dissipation of the mean square fluctuating normal vorticity in Fig. 4c is related to the radial diffusion of normal vorticity.

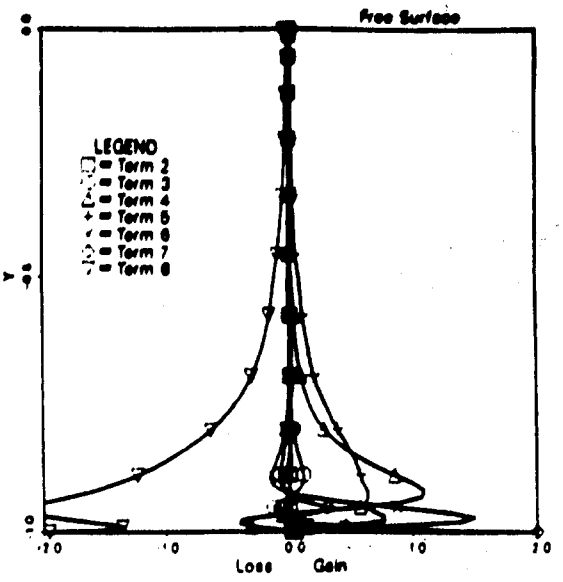

Fig. 3. The terms of Eq. 8.

Also apparent in Figs. 4b-d are the differences in the characteristics of the turbulent production and the transport of enstrophy between the cases of the horizontal vorticity and the vertical vorticity. With the exception of the mean and mixed production terms (4) and (6) the horizontal terms are similar. In the upper 1/3 of the channel, the turbulent production of enstrophy contributes positively, exhibiting a generally slow decline with increasing distance from the solid wall. However in the layer $-0.05 \geq y \geq -0.1$ the decline stops, and at least for the transverse component of enstrophy, there is a slight increase in production. Since Ω_1 and Ω_3 approach zero at the shear free boundary, the production of these components of enstrophy must also approach zero. The non-zero turbulent production of the normal component of enstrophy at the surface is a result of the shear-free boundary and a normal strain field, which will be discussed later.

The production term (5) is further separated into the various stretching and rotation components in Fig. 5. For all three enstrophy components the production due to stretching dominates. For the stretching terms to be relevant, there must be some strain aligned with the vorticity. While this strain is not accounted for by the existence of the anti-parallel image vortex, numerical experiments involving interacting vortex rings or vortex tubes indicate a rapid increase in the component of strain aligned with the vorticity during the vortex reconnection. A similar

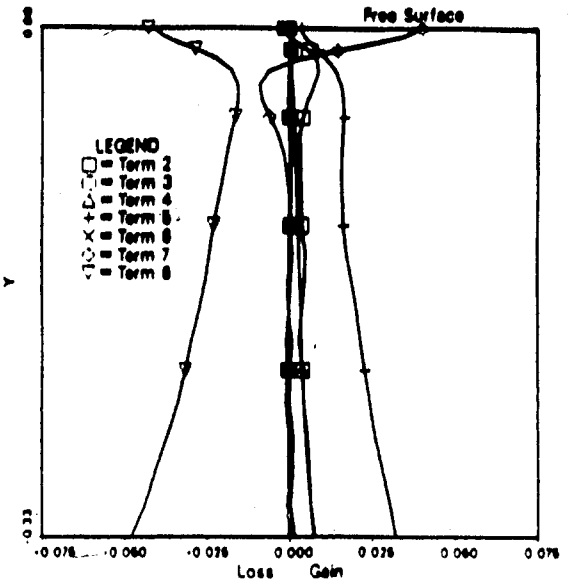

Fig. 4a. Enstrophy balance in a turbulent open channel flow near the free surface.

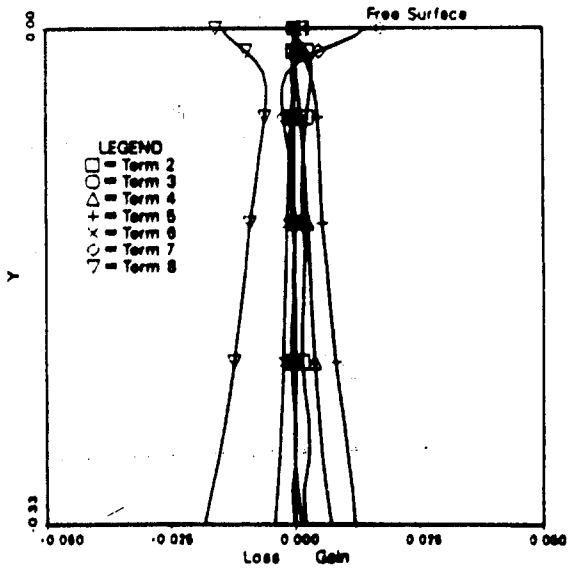

Fig. 4b. Mean square fluctuating axial vorticity balance in a turbulent open channel flow near the free surface.

process may be relevent when the horizontal components of vorticity approach the top surface. The flow field transporting the vorticity to the free surface may also be responsible for the strain.

Although the rotation terms are small and declining as the surface is approached, the terms representing the rotation of vorticity from the axial to the transverse direction and from the transverse to the axial have small increases near the boundary. This may be due to the rotation of small eddies, having vorticity components parallel to the surface by large eddies.

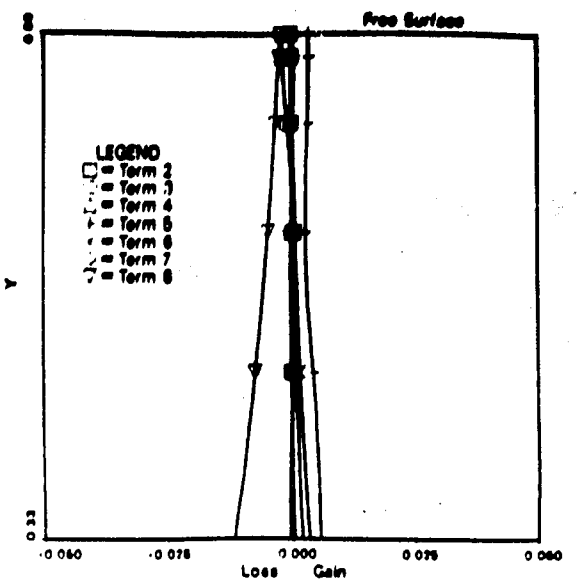

Fig. 4c. Mean square fluctuating normal vorticity balance in a turbulent open channel flow near the free surface.

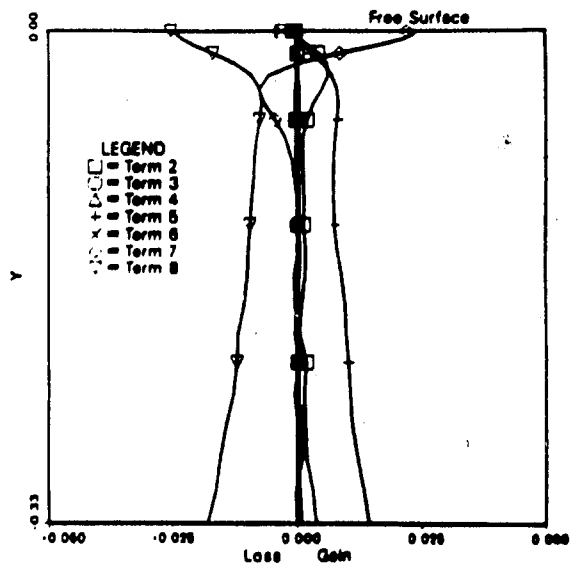

Fig. 4d. Mean square fluctuating transverse vorticity balance in a turbulent open channel flow near the free surface.

The enstrophy balance in the vertical (x_2) direction shows the effect of attachment of the normal vorticity to the free surface. The turbulent production of $\overline{\omega_2\omega_2}$ varies slightly in the upper 1/3 of the channel. However, as can be seen in Fig. 5 the production mechanism changes with increasing distance from the shear-free boundary. Near the surface, $x_2 \geq -0.0$ the stretching of the vorticity is important. Below ($x_2 \leq -0.08$) the gain in enstrophy is due to rotation of the fluctuating vorticity field, and stretching has become negligible. The source of the strain near the free-surface is probably the flow induced by the low pressure within the vorticity attached to the surface

From figure 5, it is apparent that the term in Eq. 8 most responsible for the production of enstrophy is transverse stretching of transverse vorticity, $\omega_3\omega_3\frac{\partial u_3}{\partial x_3}$. Figure 6 is a plot of this property for the plane $x_2 = -0.05$. The turbulent structures or events responsible for generating this component of the enstrophy are localized and intense. The contour intervals are $10\omega_3\omega_3\frac{\partial u_3}{\partial x_3}$. To more clearly identify the structures associated with the localized production, histograms of the level of production by turbulent stretching have been determined and are contained in Leighton[7], *et.al.* From the histograms it was determine that, at this plane ($x_2 = -0.05$) that approximately $3-6\%$ of the area was responsible for $30-60\%$ of the turbulent enstrophy production. This behavior is typical for for all nine components of term (5), Eq. 8. This conclusion was verified by calculating the skewness and flatness for these production terms. For each of the nine cases the skewness and flatness factors were large ($10-10^2$ for skew and 10^2-10^4 for flatness).

Based on the observation of production events local in space, and the behavior of the average fluctuating vorticity, two models of the interaction of vorticity with the surface were developed.

6.1 Two models for the production events

The two proposed models of the interaction of vorticity with the free surface can be described as 'the spin model' and 'the splat model'. These models are similar to and have been infleuenced by the models presented by Koh and Bradshaw[8] and Hunt[9]. Although the names are meant to be suggestive of the kinematics of the enstrophy producing events, the models are similar to the models by the same name for the pressure source terms described in Ref. 9.

In the 'spin' model, a vortical structure originating in the buffer layer, tilts downstream and is attached to the free surface in a quasi-stable configuration. This model is relevent when discussing the vertical component of enstrophy. These structures, which can be liken to vortex tubes connected to the free surface have been observed in flow visualizations of the DNS dataset of the open channel flow. Within these vortex tubes there is a significant 'down draft'. It is conjectured that this down draft is responsible for the transport of enstrophy away from the surface and provides the strain necessary to maintain these structures. Were it not for these down drafts, and the vorticity intensification they provide, these vortical structures would eventually diffuse and cancel.

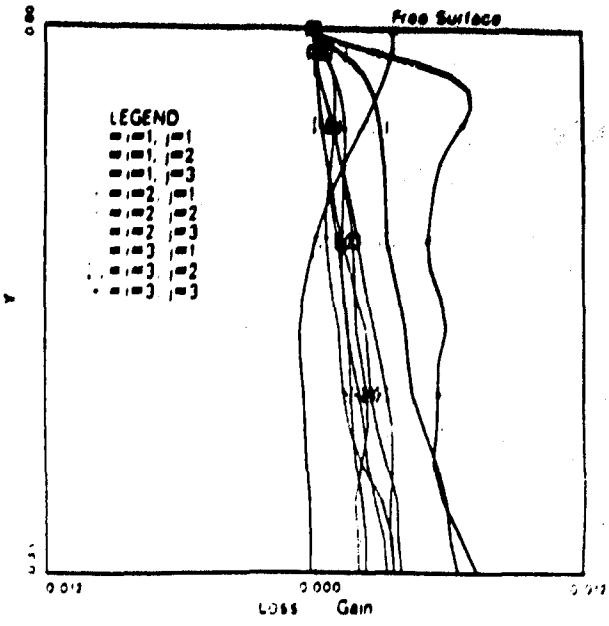

Fig. 5. Turbulent production of fluctuationg enstrophy by stretching (heavy lines) and rotation (light lines), $\overline{\omega_i\omega_j\frac{\partial u_3}{\partial x_j}}$.

The eventual diffusion has been seen in a simulation of vortex reconnection in which there was no down draft.[10] In this case there was radial diffusion of vorticity from the core near the intersection of the vortex ring and the shear-free surface.

In the 'splat' model a volume of fluid 'containing' vorticity impacts the free surface, leading to stretching, intensification and cancellation of vorticity. The fluctuating normal velocity field promotes the increase of horizontal component enstrophy near the free surface by two mechanisms: transport and vortex stretching. Due to the large gradient in $\overline{\omega_1\omega_1}$ and $\overline{\omega_3\omega_3}$ near the top boundary, the vertical velocity fluctuations provide an efficient means of transporting vorticity to the free surface. As the turbulent eddy approaches the top boundary the vertical component is deflected into the horizontal direction. During the 'splat' event, the vorticity contained in a turbulent eddy interacting with the top surface will be rotated parallel to the boundary and stretched. The vorticity in the fluid near the free surface will be subjected to a large strain and will have a large gradient due to the proximity of its reflected image. This leads to increased production of fluctuating enstrophy by the fluctuating velocity fields and to large enstrophy dissipation or vorticity cancellation. Other details about this type of model can be found in Ref. 9.

7. Conditional Sampling and Ensemble Averaging

To verify that the two models are qualitatively correct, the open channel flow was conditionally sampled on the plane $x_2 = -0.05$. The condition used was that the local value of the enstrophy production by vortex stretching (rotation was not considered) exceeded the mean value by a factor of ten, and that the production was a local maximum. The enstrophy production at the locations determined by the first condition accounted for approximatedly 50% of the production by stretching and rotation, but only about 2% of the area. For the spanwise component, $\omega_3\omega_3\frac{\partial u_3}{\partial x_3}$, only detected events with negative vorticity were considered. There were approximately an order of magnitude more events with negative vorticity contributing to the turbulent production of spanwise enstrophy than events with positive vorticity. For the remaining components, only events with positive vorticity were considered. In this case there were as many positive as negative vortical events detected.

Certain properties associated with these events have been ensemble averaged and are shown in figures 7 – 10. The properties are averaged on a vertical line through the detected events. The ensemble averaged vorticity, shown in Fig. 7 are larger than those shown in Fig. 1, almost by a factor of ten, an indication that these events are substantial contributors to the rms vorticity.

7.1 The Spin Event

As discussed above the spin model involves a vortical structure, like a vortex tube attached to the free surface and extending into the buffer layer. The existance of substantial ensemble-averaged vertical vorticity in regions far from the free surface, as seen in Fig. 7 supports the conceptual model of an attached vortex tube.

Fig. 8 is the ensemble-averaged vertical velocity. In the case of the normal component of enstrophy, the negative velocity will stretch the attached vertical vorticity. This is the down-draft within the vortex tube mentioned earlier. The peak negative velocity occurs at $x_2 \approx -0.15$. The strain rates $\frac{\partial u_i}{\partial x_i}$ are shown in Fig. 9. The peak in the normal strain occurs at the surface, again consistant with the proximity of the vortex stretching with the free surface. The strain and the resulting vortex stretching are negative for $x_2 < -0.15$. This may be due in part to the tilting of the vortical structure in the main part of the flow

The final figure is the rate of dissipation of enstrophy for each of the components. The normal vorticity is largely unaffected by its image and has a low level of dissipation. Due to this small dissipation, it is conjectured that these events will have a longer duration than the 'splat' events.

7.2 The Splat Event

Although the conditionally sampled results are consistant with both the model and the RMS vorticity distributions, they donot explain the greater intensity of the ω_3 components. The location of the maximum transverse vorticity is above the conditioning plan $y = -0.05$ while the maximum for the axial vorticity is below. This characteristic and the amplitude of the maximum are consistant with their rms values

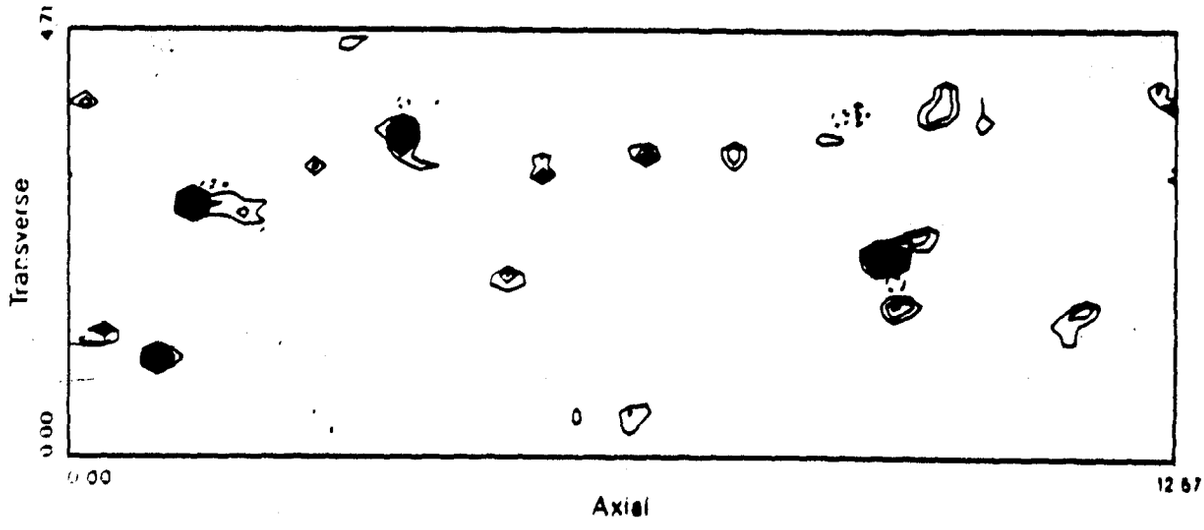

Fig. 6. Enstrophy production due to transverse stretching of transverse vorticity ($\omega_3\omega_3\frac{\partial u_3}{\partial x_3}$). Planview of plane $y = -0.05$. Contours are for $\omega_3\omega_3\frac{\partial u_3}{\partial x_3} = 10\overline{\omega_3\omega_3\frac{\partial u_3}{\partial x_3}}$.

Fig. 8 is the vertical velocity associated with these events. For the rising turbulent eddy of the model the vertical velocity is positive, resulting in a 'splat' at the surface. The strain rates $\frac{\partial u_i}{\partial x_i}$ are shown in figure 9. The transverse strain is larger is the axial strain. This is consistent with the larger transverse turbulent production and vorticity.

Fig. 10 is the rate of dissipation of enstrophy for each of the components. The terms in x_1 and x_3 direction are similar. The dissipation occurs very close to the boundary and is very intense: approximately an order of magnitude larger than the mean value. Due to the reflective nature shear-free boundary there exists an image vorticity across the boundary resulting in annihilation of vorticity near the shear-free boundary.

8. Conclusions

The enstrophy balance equations have been evaluated for a direct numerical simulation of turbulent open channel flow. The free surface has been modeled as a shear-free boundary. Near the free surface there are two dominate sources of enstrophy: Transport due to velocity fluctuations and production due to the vortex stretching and rotation by the velocity fluctuations. At the free surface, diffusion is the dominate source of enstrophy. The gains in enstrophy are balanced by enstrophy dissipation. When the components of the total enstrophy are considered individually, the components parallel to the surface, ($\overline{\omega_1\omega_1}$ and $\overline{\omega_3\omega_3}$) are found to be responsible for the variation in the balances near the surface. The balance equations for $\overline{\omega_2\omega_2}$ show little variation near the surface.

Two models, referred to as the 'spin' and 'splat' models can be used to explain this behavior. The splat model is similar to the model discussed in Hunt[6] in which an eddy is swept to the surface. The resulting redistribution of normal momentum into horizontal momentum will stretch and intensify any vorticity transported in the eddy. Due to the image vorticity resulting from the reflective nature of the free surface, the intense vorticity will quickly cancel with its image and the enstrophy dissipation will be enhanced.

Fundamental to the 'spin' model is a stable vortical structure originating in the buffer layer and extending to the free surface. The mild variation of the normal balance is a result of the quasi-stable nature of the attached structure. Without close anti-parallel image vorticity, these structures do not dissipate quickly. The downflow within these vortical structures result in sufficient strain to maintain the vorticity against the effects of viscous diffusion.

A large portion of the production of enstrophy near the free surface is due to these highly localized intense events. The area responsible for this production is very small. Approximately 3 – 6% of the area on the plane $x_2 = -0.05$ is responsible for 30 – 60% of the production. Conditionally sampling and ensemble averaging the production events verified that their characteristics are consistant with the proposed models.

Acknowledgements

This work is supported by the Naval Research Laboratory as part of the Fluid Dynamics Task Area. The simulations were performed at the Naval Research Laboratory.

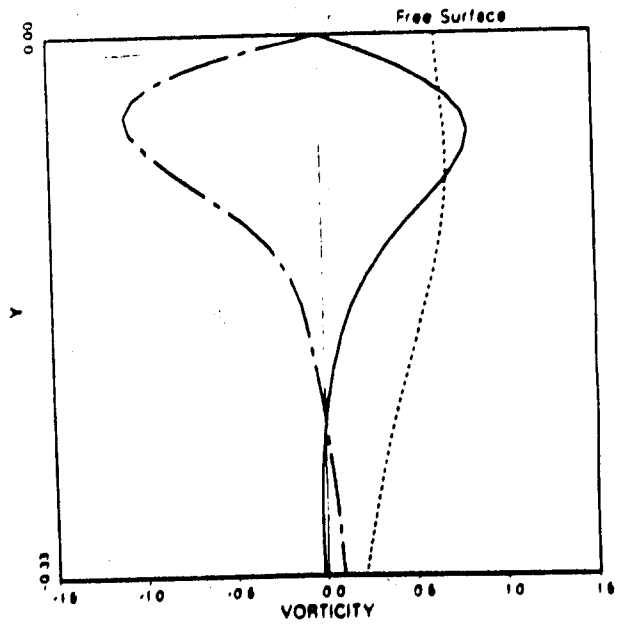

Fig. 7. Ensemble averaged vorticity, conditioned by the requirement that $\omega_i\omega_i\frac{\partial u_i}{\partial x_i} \geq 10\overline{\omega_i\omega_i\frac{\partial u_i}{\partial x_i}}$.
——, $\langle\omega_1\rangle$; – – –, $\langle\omega_2\rangle$; - - - -, $\langle\omega_3\rangle$.

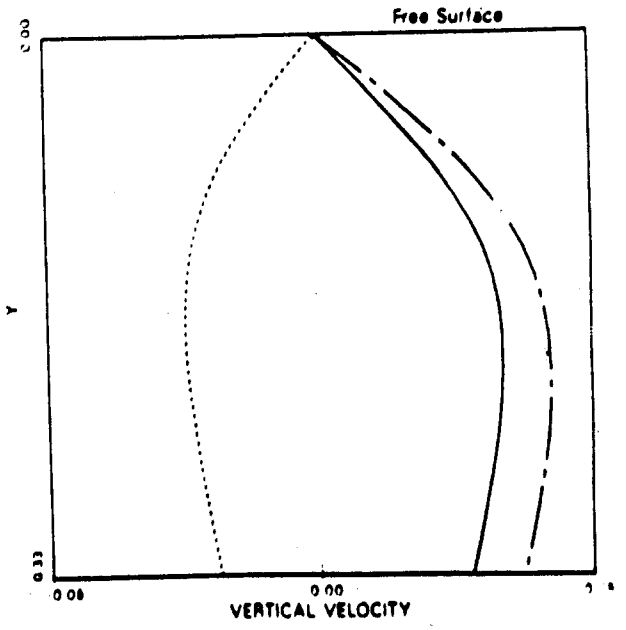

Fig. 8. Ensemble averaged vertical velocity.
——, $i = 1$; – · –, $i = 2$; - · - ·, $i = 3$.

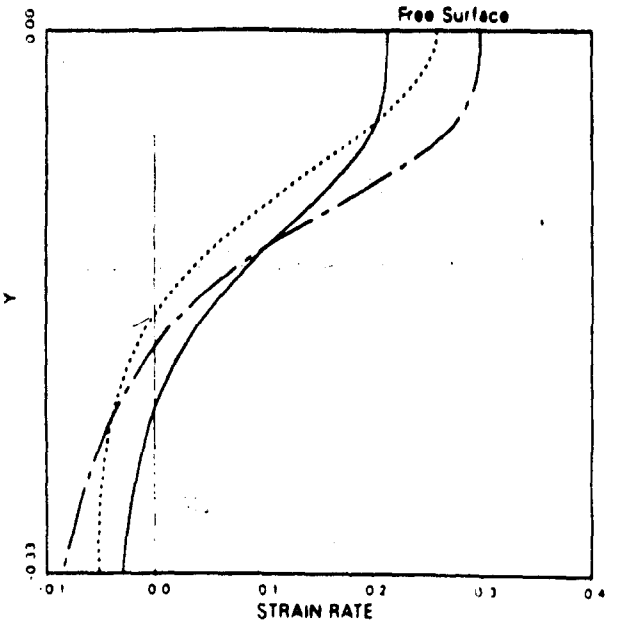

Fig. 9. Ensemble averaged strain.
—, $\langle \frac{\partial u_1}{\partial x_1} \rangle$; - - -, $\langle \frac{\partial u_2}{\partial x_2} \rangle$; ·····, $\langle \frac{\partial u_3}{\partial x_3} \rangle$.

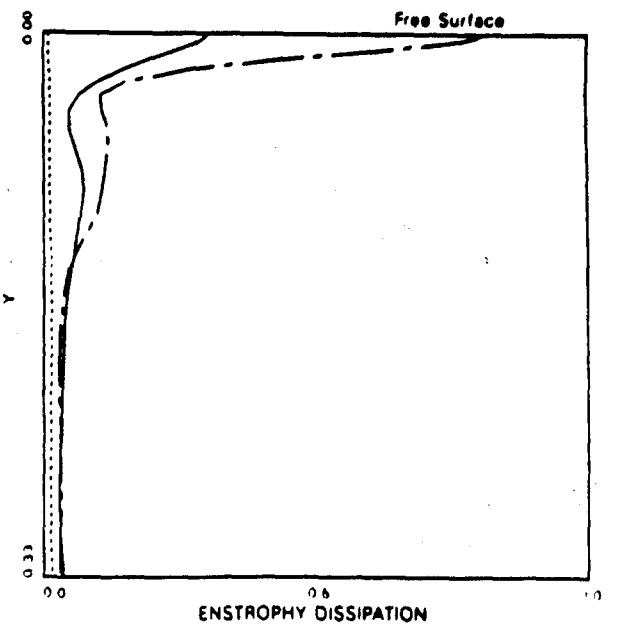

Fig. 10. Ensamble averaged dissipation of enstrophy.
—, $i = 1$; - - -, $i = 2$; ·····, $i = 3$.

References

[1] Hinze, J.O., 1975 *Turbulence*. McGraw-Hill, New York

[2] Orszag, S.A., and Patera, A.T., 1981 Subcritical Transition to Turbulence in Planar Shear Flows in *Transition and Turbulence*. Academic Press, London.

[3] Kim, J., Moin, P., and Moser, R., 1987 Turbulence statistics in a fully developed channel flow at low Reynolds number. *J. Fluid Mech.*177,133.

[4] Balint, J.-L., Vukoslavcevic, P. and Wallace, J.M., 1988 The transport of enstrophy in a turbulent boundary layer. In *Proceedings of the Zarif Memorial Internation Seminar on Wall Turbulence.*

[5] Tennekes, H. and Lumley, J.L., 1972 *A First Course In Turbulence*. The MIT Press, Cambridge, Mass.

[6] Batchelor, G.K., 1967 *An Introduction To Fluid Dynamics*. Cambridge University Press, Cambridge, England.

[7] Leighton, R.I., Swean, T.F., Handler, R.A. and Swearingen, J.D., 1991 Direct simulation of low Reynolds number open channel flow. In preparation for submittal to *Physics of Fluids*.

[8] Bradshaw, P. and Koh, Y.M., 1981 A note on Poisson's equation for pressure in a turbulent flow. *Physics of Fluids*. **24**, 777.

[8] Hunt, J.C.R. 1984 Turbulence structure and turbulent diffusion near gas-liquid interfaces. in *Gas Transfer at Water Surfaces*. D. Reidel Pub Co.

[10] Leighton, R.I. and Swean, T.F., 1991 The interaction of a vortex ring with a shear-free boundary. In preparation for submittal to *Physics of Fluids*.